

# Lawrence Berkeley National Laboratory

## Lawrence Berkeley National Laboratory

### **Title**

An asixymmetric diffusion experiment for the determination of diffusion and sorption coefficients of rock samples

### **Permalink**

<https://escholarship.org/uc/item/8dx1t5mn>

### **Author**

Takeda, M.

### **Publication Date**

2011-03-04

Peer reviewed

## **An axisymmetric diffusion experiment for the determination of diffusion and sorption coefficients of rock samples**

M. Takeda<sup>a</sup>, T. Hiratsuka<sup>a</sup>, K. Ito<sup>a</sup>, S. Finsterle<sup>b</sup>

<sup>a</sup> National Institute of Advanced Industrial Science and Technology (AIST), Higashi 1-1-1, Central 7, Tsukuba, Ibaraki 305-8567, Japan

<sup>b</sup> Lawrence Berkeley National Laboratory, Earth Sciences Division, 1 Cyclotron Rd., MS 90-1116, Berkeley, CA 94720, United States

### **Abstract**

Diffusion anisotropy is a critical property in predicting migration of substances in sedimentary formations with very low permeability. The diffusion anisotropy of sedimentary rocks has been evaluated mainly from laboratory diffusion experiments, in which the directional diffusivities are separately estimated by through-diffusion experiments using different rock samples, or concurrently by in-diffusion experiments in which only the tracer profile in a rock block is measured.

To estimate the diffusion anisotropy from a single rock sample, this study proposes an axisymmetric diffusion test, in which tracer diffuses between a cylindrical rock sample and a surrounding solution reservoir. The tracer diffusion between the sample and reservoir can be monitored from the reservoir tracer concentrations, and the tracer profile could also be obtained after dismantling the sample. Semi-analytical solutions are derived for tracer concentrations in both the reservoir and sample, accounting for an anisotropic diffusion tensor of rank two as well as the dilution effects from sampling and replacement of reservoir solution.

The transient and steady-state analyses were examined experimentally and numerically for different experimental configurations, but without the need for tracer profiling. These experimental configurations are tested for in- and out-diffusion experiments using Koetoi and Wakkanai mudstones and Shirahama sandstone, and are scrutinized by a numerical approach to identify favorable conditions for parameter estimation.

The analysis reveals the difficulty in estimating diffusion anisotropy; test configurations are proposed for enhanced identifiability of diffusion anisotropy. Moreover, it is demonstrated that the axisymmetric diffusion test is efficient in obtaining the sorption parameter from both steady-state and transient data, and in determining the effective diffusion coefficient if isotropic diffusion is assumed. Moreover, measuring reservoir concentrations in an axisymmetric diffusion experiment coupled with tracer profiling may be a promising approach to estimate of diffusion anisotropy of sedimentary rocks.

**Keywords:** diffusion experiment, anisotropic diffusion, sorption, axisymmetric analytical model, analytical solution, inverse analysis

## 1. Introduction

In many industrial countries, deep sedimentary formations are potential candidates for disposal of radioactive wastes due to their very low hydraulic conductivities and efficient retention properties. These formations are also natural barriers for CO<sub>2</sub> sequestration due to their stratigraphic seals impeding fluid migration. In the water-saturated, advection-limited rock matrix, the migration of species dissolved in the aqueous phase is mainly dominated by diffusion, in addition to the sorption onto or reaction with the solid phase. Therefore, the properties of sedimentary rocks relevant to the diffusion-dominated transport are of fundamental importance for performance assessment of geological disposal projects.

Sedimentary rocks generally possess preferential orientations of the pore space (Nakashima et al., 2008; Wenk et al., 2008). In the aqueous phase within the low-permeability rock matrix, the species migrate through the porewater by their random motion along the connected pore structure, leading to directional, anisotropic diffusion behavior. Such directional diffusivities of sedimentary rocks are typically described by diffusion tensor of rank two (e.g., Nakashima et al., 2008).

In the context of geological disposal, the diffusion anisotropy of clayey rocks has received considerable attention in recent years. Extensive studies on the Opalinus clay (Switzerland) and Callovo-Oxfordian clay (France) have shown that the diffusion in these media is prominent in the direction parallel to the bedding plane (e.g., Van Loon et al., 2004a, 2004b; García-Gutiérrez et al., 2006, 2008; Samper et al., 2008a). Numerical models of

in-situ experiments performed in these areas have treated directional diffusivities as a diffusion tensor of rank two (e.g., Wersin et al., 2004; Yllera et al., 2004).

The diffusion anisotropy of the clayey rocks has been investigated mainly by in-situ and laboratory diffusion experiments. In-situ experiment can determine the directional diffusivities under natural conditions on the field scale. However, experimental times are very long, e.g., up to several hundred days. Moreover, these in-situ experiments need to be supplemented with laboratory experiments to properly interpret the field data (Wersin et al., 2004; Yllera et al., 2004). According to Samper et al. (2008b), the interpretation of in-situ diffusion experiments may also be complicated by several non-ideal effects caused by the presence of a sintered filter, a gap between the filter and the borehole wall, and an excavation disturbed zone.

To overcome these non-ideal effects, García-Gutiérrez et al. (2006) developed a large-scale laboratory diffusion experiment by tracer profiling of a cylindrical block (0.3×0.3 m), and evaluated the diffusion anisotropy of the Opalinus clay using HTO,  $^{36}\text{Cl}^-$ , and  $^{85}\text{Sr}$ . The diffusion anisotropy estimated from HTO and  $^{36}\text{Cl}^-$  were consistent with those evaluated by Van Loon et al. (2004a) from through-diffusion experiments. García-Gutiérrez et al. (2008) applied the same experimental configuration to the Callovo-Oxfordian clay, and Samper et al. (2008a) examined the reliability of estimating parameters in these experiments.

Laboratory experiments enable the investigation of diffusion anisotropy under well-controlled conditions. Van Loon et al. (2004a) evaluated the diffusion anisotropy of Opalinus clay under 1D mechanical stresses by 1D and radial through-diffusion experiments using HTO,  $^{36}\text{Cl}^-$ , and  $^{22}\text{Na}^+$ . The derived properties have been successively applied to the interpretation of in-situ experiments and the performance confirmation of newly developed experiments measuring diffusion anisotropy (Soler et al., 2008; García-Gutiérrez et al., 2006).

Overall, laboratory diffusion experiments are essential for estimating the diffusion anisotropy and are necessary for interpreting in-situ experiments. However, tracer profiles obtained from conventional diffusion experiments are often uninformative regarding the anisotropy of the diffusion process. If tracer profiles are measured at the end of a diffusion experiment but without monitoring the transient tracer diffusion process, separate diffusion experiments for the same material and tracer are necessary to deduce the appropriate time

for tracer profiling (García-Gutiérrez et al., 2006). Moreover, the representativeness of the estimated diffusion anisotropy remains questionable. If using through-diffusion experiments, directional diffusivities are essentially estimated from separate experiments using different rock samples.

This study proposes an axisymmetric diffusion test capable of estimating diffusion anisotropy from a single rock sample. In the experiment, tracer diffuses between a cylindrical rock sample and a surrounding solution reservoir. The tracer diffusion between the sample and reservoir can be monitored by measuring tracer concentrations in the reservoir. In addition, tracer profiles could be obtained after dismantling the sample. For the interpretation of the reservoir tracer concentration changes and the tracer profiles in the rock sample at the end of the experiment, an axisymmetric analytical model is developed, and semi-analytical solutions are derived that account for directional diffusivities of the diffusion tensor of rank two with zero off-diagonal elements for both in- and out-diffusion experiments. Moreover, the dilution effect caused by the replacement of reservoir solution taken for chemical analysis is included in the model, so are the effects of tracer addition when multiple experiments are conducted in sequence.

Similar experimental setups and analytical models have been presented in earlier studies. Skagius and Neretnieks (1988) performed in-diffusion experiments using cylindrical rock samples of biotite gneiss (with a diameter of 42 mm and a length of 32 or 40 mm), using cesium and strontium as the tracers. The tracer profiles were interpreted using a 1D diffusion model along the sample axis, as the diffusive length in radial direction was relatively short. Ibaraki (2001) proposed a 3D in-diffusion test for cuboidal rock samples, and also derived the associated semi-analytical solutions using an analytical model that is similar to that presented in our study. In the experiments, the changes of ionic tracer concentration were measured by an electric conductivity sensor, and were interpreted assuming isotropic diffusion. These studies suggest that tracer profiling is feasible on small samples if the experiments are terminated at an appropriate time, and that the reservoir tracer concentration analysis method is suitable to estimate (isotropic) diffusion and sorption parameters despite the increased dimensionality of tracer diffusion. However, the ability of the reservoir concentration analysis method to estimate directional diffusivities along with the sorption parameter has not yet been demonstrated. One of the objectives of this study is to evaluate whether reservoir concentration data collected during an

axisymmetric diffusion experiment contain sufficient information to allow the reliable determination of anisotropic diffusion and sorption parameters.

In this study, the axisymmetric diffusion test is applied to determine the diffusion and sorption parameters for three types of sedimentary rocks, Wakkanai and Koetoi mudstone and Shirahama sandstone. In the experiments, changes in reservoir tracer concentration are interpreted by both isotropic and anisotropic diffusion models. The steady-state analyses also provide independent estimates of sorption parameters. The feasibility of estimating the directional diffusivities is further examined using synthetic data. In the synthetic, transient analyses, sensitivity, uniqueness, correlation structure, and estimation uncertainty are investigated using the anisotropic model for a large variety of experimental conditions and a wide range of potential diffusion properties. Finally, practical limitations and possible applications of the axisymmetric diffusion test are discussed.

## **2. Test method and mathematical formulation**

### 2.1. Experimental procedures

Fig. 1 illustrates axisymmetric diffusion experiments to be performed without tracer profiling. Before the experiment, the rock sample is immersed in a solution to obtain a uniform tracer distribution in both the porewater and the reservoir. Moreover, a vacuum is applied to evacuate air that is potentially entrapped in the pores. The diffusion experiment starts by replacing the reservoir solution with a solution of a different tracer concentration. If the tracer concentration of the replacement solution is higher than that of the porewater, the tracer diffuses into the rock sample from the solution reservoir (in-diffusion experiment). If the tracer concentration of the replacement solution is lower than that of the reservoir, the tracer diffuses out of the rock sample (out-diffusion experiment). The reservoir tracer concentrations are measured by sensors, such as ion-selective or conductivity electrodes, and/or by chemical analysis of the reservoir solution. If the reservoir solution is sampled for concentration measurement, tracer-free solution is added in the same amount as the sampling volume. Analytical solutions are used to infer the diffusion and sorption parameters from the measured tracer concentrations.

## 2.2. Analytical model

Assuming a linear sorption isotherm, the axisymmetric diffusion of a tracer solute in a porous medium is described as (e.g., Samper et al., 2008)

$$\alpha \cdot \frac{\partial C}{\partial t} = D_{er} \cdot \left( \frac{\partial^2 C}{\partial r^2} + \frac{1}{r} \cdot \frac{\partial C}{\partial r} \right) + D_{ez} \cdot \frac{\partial^2 C}{\partial z^2}, \quad 0 \leq r < r_o, \quad -\frac{L}{2} < z < \frac{L}{2}, \quad 0 < t < +\infty \quad (1)$$

where  $C$  is the tracer concentration in the porewater [ $\text{ML}^{-3}$ ],  $t$  is the time [ $\text{T}$ ],  $r$  and  $z$  are the radial and vertical coordinates [ $\text{L}$ ],  $r_o$  and  $L$  are the radius and length of the sample [ $\text{L}$ ],  $D_{er}$  and  $D_{ez}$  are the effective diffusion coefficients in the radial and vertical directions [ $\text{L}^2\text{T}^{-1}$ ], and  $\alpha$  is the capacity factor [-], which can be expressed as the sum of the total porosity and volume sorption coefficient,  $\alpha = \phi + \rho_b \cdot K_d$ , in which  $\phi$  is the total porosity [-],  $\rho_b$  is the dry bulk density of the porous medium [ $\text{ML}^{-3}$ ], and  $K_d$  is the distribution coefficient [ $\text{M}^{-1}\text{L}^3$ ]. The boundary conditions at the external surface of the rock sample at time  $t$  are given by

$$C(r_o, z, t) = C_R(t), \quad C(r, L/2, t) = C_R(t) \quad \text{and} \quad C(r, -L/2, t) = C_R(t) \quad (2)$$

where  $C_R$  is the tracer concentration in the reservoir [ $\text{ML}^{-3}$ ]. Before the experiment, the tracer concentration equilibrates between the porewater and the reservoir:

$$C(r, z, t) = C_R(t) = C_{in}, \quad 0 \leq r < r_o, \quad -L/2 < z < L/2, \quad t < 0 \quad (3)$$

where  $C_{in}$  is the tracer concentration before the experiment [ $\text{ML}^{-3}$ ]. The diffusion experiment starts by replacing the reservoir solution with an equal volume of a solution of a different tracer concentration. The reservoir tracer concentration at the start of the experiment,  $t=0$ , is expressed as

$$C_R(0) = \frac{V_R \cdot C_{in} - V_{s,0} \cdot (C_{in} - C_{tr,0})}{V_R} \quad (4)$$

where  $V_R$  is the reservoir volume [ $\text{L}^3$ ],  $C_{tr,0}$  [ $\text{ML}^{-3}$ ] is the tracer concentration, and  $V_{s,0}$  [ $\text{L}^3$ ] is the volume of the replacement solution. In in-diffusion and out-diffusion experiments,  $C_R(0)$  is higher and lower than  $C_{in}$ , respectively. From mass balance considerations, the reservoir tracer concentration at time  $t > 0$  is expressed as (e.g., Ibaraki, 2001)

$$V_R \cdot \frac{dC_R}{dt} = -2 \cdot \pi \cdot r_o \cdot D_{er} \cdot \int_{-L/2}^{L/2} \frac{\partial C}{\partial r} \Big|_{r=r_o} dz + 2 \cdot \pi \cdot D_{ez} \cdot \left( - \int_0^{r_o} \frac{\partial C}{\partial z} \Big|_{z=L/2} r dr + \int_0^{r_o} \frac{\partial C}{\partial z} \Big|_{z=-L/2} r dr \right) + \sum_{i=1}^M V_{s,i} \cdot (C_{tr,i} - C_R(t_i)) \cdot \delta(t - t_i) \quad (5)$$

where  $M$  is the number of solution samples taken,  $t_i$  is the time of the  $i$ -th solution sampling,  $C_R(t_i)$  and  $C_{tr,i}$  are the tracer concentrations of the  $i$ -th sample and replacement solutions, respectively,  $V_{s,i}$  is the volume of the  $i$ -th sample and replacement solutions, and  $\delta$  is the Dirac delta function. The three integral terms on the right-hand side represent diffusion fluxes through the external surface of the rock sample. The last term on the right-hand side represents the solution replacements at time  $t_i$ . If tracer-free solutions are used as the replacement solution,  $C_{tr,i}$  becomes zero. If the reservoir solution is not sampled, i.e., if the reservoir tracer concentrations are measured by in-situ sensors, the last term on the right-hand side of Eq. (5) is irrelevant.

### 2.3. Transient and steady-state analytical solutions

The problem defined by Eqs. (1) to (5) is solved by applying the Laplace and Fourier sine transforms with respect to time and the spatial variables, respectively (e.g., Ibaraki, 2001). For simplicity, the analytical solutions are expressed using the following dimensionless variables:

$$\rho = \frac{r}{r_o}, \quad \xi = \frac{z}{r_o} \cdot \frac{1}{\sqrt{\kappa}}, \quad \tau = \frac{D_{er} \cdot t}{\alpha \cdot r_o^2}$$

$$c(\rho, \xi, \tau) = \frac{C - C_{in}}{C_R(0) - C_{in}}, \quad c_R(\tau) = \frac{C_R - C_{in}}{C_R(0) - C_{in}}, \quad c_{tr,i} = \frac{C_{tr,i} - C_{in}}{C_R(0) - C_{in}} \quad (6)$$

$$\lambda = \frac{L}{2 \cdot r_o} \cdot \frac{1}{\sqrt{\kappa}}, \quad \beta_R = \frac{V_R}{\pi \cdot r_o^2 \cdot L \cdot \alpha}, \quad \beta_{s,i} = \frac{V_{s,i}}{\pi \cdot r_o^2 \cdot L \cdot \alpha}$$

where  $\rho$  and  $\xi$  are the normalized distances in the radial and vertical coordinates,  $\tau$  is the normalized time,  $c$  and  $c_R$  are the normalized tracer concentrations of the porewater and the reservoir, respectively,  $c_{tr,i}$  is the normalized tracer concentration of the  $i$ -th replacement solution at normalized sampling time  $\tau_i$ ,  $\ell$  is the aspect ratio of the rock sample in the dimensionless scale,  $\hat{V}_R$  and  $\hat{V}_{s,i}$  are the normalized volumes of the reservoir and replacement solutions, respectively, and  $\beta = D_{ez}/D_{er}$  represents the degree of the diffusion anisotropy between the radial and vertical direction. If  $\beta$  is one, the analytical model



becomes an isotropic diffusion model. is hereafter referred to as the diffusion anisotropy ratio.

The transient analytical solution for the reservoir tracer concentration can be derived in the Laplace domain as follows:

$$\bar{c}_R(p) = \frac{\beta_R + \sum_{i=1}^M \beta_{s,i} \cdot (c_{tr,i} - c_R(\tau_i)) \cdot \exp(-p \cdot \tau_i)}{p \cdot \left\{ \beta_R + 1 - \frac{8 \cdot p}{\lambda^2} \sum_{m=1}^{\infty} \sum_{n=1}^{\infty} (p + \psi_m^2 + \phi_n^2)^{-1} \cdot \psi_m^{-2} \cdot \phi_n^{-2} \right\}} \quad (7)$$

where  $\bar{c}_R$  is the Laplace-transformed reservoir tracer concentration,  $p$  is the Laplace transform variable,  $\psi_m = (2 \cdot m - 1) \cdot \lambda / (2 \cdot \ell)$ , and  $\phi_n$  are the roots of  $J_0(\phi) = 0$ . The transient analytical solution for the porewater tracer concentration can also be derived in the Laplace domain:

$$\bar{c}(\rho, \xi, p) = \bar{c}_R(p) \cdot \left\{ 1 - \frac{4 \cdot p}{\lambda} \sum_{m=1}^{\infty} \sum_{n=1}^{\infty} \frac{J_0(\phi_n \cdot \rho) \cdot \sin(\psi_m \cdot (\xi + \lambda))}{(p + \psi_m^2 + \phi_n^2) \cdot \psi_m \cdot \phi_n \cdot J_1(\phi_n)} \right\} \quad (8)$$

where  $\bar{c}$  is the Laplace-transformed tracer concentration of the porewater.

The reservoir tracer concentration at steady state ( $t \rightarrow \infty$ ) can be obtained by applying the final value theorem to Eq. (7) (Novakowski and van der Kamp, 1996; Ibaraki, 2001):

$$c_R(+\infty) = \frac{\beta_R + \sum_{i=1}^M \beta_{s,i} \cdot \{c_{tr,i} - c_R(\tau_i)\}}{\beta_R + 1} \quad (9)$$

In Eqs. (7) and (9), the series in the numerator is omitted if the reservoir solution is not sampled. In dimensionless form, the initial reservoir concentration,  $c_R(0)$  in Eq. (6), is by definition equal to one. Therefore, the magnitude of concentration change at steady state, i.e.,  $c_R(0) - c_R(+\infty)$ , is related to the values of  $\beta_R$  and  $\beta_{s,i}$ , which are design parameters of the experiment that can be optimized.

#### 2.4. Interpretation of experimental data

The effective diffusion coefficient(s) and the capacity factor in Eqs. (1) and (5) are the

parameters to be identified. If the steady-state reservoir tracer concentration is available, the capacity factor,  $\tau$ , can be determined from the steady-state concentration. Treating the final measured concentration  $C_R(t_M)$  as  $C_R(\infty)$ , Eq. (9) can be reformulated as:

$$\alpha = \left\{ \frac{V_R \cdot (C_R(0) - C_{in}) + \sum_{i=1}^{M-1} V_{s,i} \cdot (C_{tr,i} - C_R(t_i))}{V_R \cdot (C_R(t_M) - C_{in})} - 1 \right\} \cdot \frac{V_R}{\pi \cdot r_o^2 \cdot L} \quad (10)$$

This reduces the number of parameters that need to be determined from the transient concentration data. However, in the experiments with solution sampling, the reservoir solution is diluted with tracer-free replacement solutions after each sampling, which may make it difficult to ascertain if the experiment has reached steady state. To determine the diffusion and sorption parameters from the transient analysis of reservoir tracer concentrations, this study adopts the Levenberg-Marquardt algorithm to minimize the following objective function (e.g., Press et al., 1992):

$$S(\mathbf{x}) = \sum_{i=1}^M \left\{ \frac{C_R^*(t_i) - C_R(t_i; \mathbf{x})}{\sigma_i} \right\}^2 \quad (11)$$

where  $S$  is the sum of squared weighted residuals between measured and modeled reservoir tracer concentrations ( $C_R^*$  and  $C_R$ , respectively) at  $t_i$ ,  $\mathbf{x}$  is the vector of unknown parameters, i.e.,  $D_{er}$ ,  $\tau$  and  $D_{ez}$  (or  $\lambda$ ) for the anisotropic diffusion model, and  $\sigma_i$  is the standard deviation of the  $i$ -th measurement data. If the isotropic diffusion model is applied, i.e.,  $\lambda = 1$ , the unknown parameters become  $D_{er}$  and  $\tau$ . For the anisotropic diffusion model, we use the diffusion anisotropy ratio  $\lambda$  as an additional unknown parameter instead of the vertical effective diffusion coefficient,  $D_{ez}$ .

Minimization of Eq. (11) requires calculation of the reservoir tracer concentrations and their sensitivities with respect to the unknown parameters. The reservoir tracer concentration can be calculated from Eq. (7) by using the numerical inversion of the Laplace transform via the de Hoog algorithm (Hollenbeck, 1998; Ibaraki, 2001, and references therein). The sensitivities are expressed as follows (Kabala, 2001):

$$\frac{\partial C_R}{\partial D_{er}} = \frac{C_R(0) - C_{in}}{D_{er}} \cdot \tau \cdot \frac{\partial c_R}{\partial \tau} \quad (12)$$

$$\frac{\partial C_R}{\partial \alpha} = -\frac{C_R(0) - C_{in}}{\alpha} \cdot \left( \tau \cdot \frac{\partial c_R}{\partial \tau} + \beta_R \cdot \frac{\partial c_R}{\partial \beta_R} + \sum_{i=0}^N \beta_{s,i} \cdot \frac{\partial c_R}{\partial \beta_{s,i}} \right) \quad (13)$$

$$\frac{\partial C_R}{\partial \kappa} = -\frac{C_R(0) - C_{in}}{\kappa} \cdot \frac{\lambda}{2} \cdot \frac{\partial c_R}{\partial \lambda} \quad (14)$$

The partial derivatives to  $\hat{\downarrow}_R$ ,  $\hat{\downarrow}_{s,i}$ , and  $\ell$  are calculated by numerically inverting the partial derivatives of the Laplace domain solution with respect to the unknown parameters. The product of  $\hat{\downarrow}$  and the derivative to  $\hat{\downarrow}$  in Eqs. (12) and (13) is calculated by numerically inverting its Laplace transformation:

$$\tau \cdot \frac{\partial c_R}{\partial \tau} = -L^{-1} \left[ c_R(p) + p \cdot \frac{\partial c_R}{\partial p}(p) \right] (\tau) \quad (15)$$

To estimate the uncertainty in the parameters determined from the steady-state and transient analyses using Eqs. (10) and (11), we evaluate the estimation covariance matrix assuming linearity and normally distributed measurement errors.

For the steady-state analysis using Eq. (10), the variance of the estimated capacity factor,  $\sigma_\alpha^2$ , is approximated by

$$\sigma_\alpha^2 = \sum_{i=1}^{M-1} \left\{ \left( \frac{\partial \alpha}{\partial C_R(t_i)} \right)^2 \cdot \sigma_i^2 \right\} + \left( \frac{\partial \alpha}{\partial C_R(t_M)} \right)^2 \cdot \sigma_M^2 \quad (16)$$

The partial derivatives of the capacity factor with respect to  $C_R(t_i)$  and  $C_R(t_M)$  in Eq. (16) can be derived from Eq. (10).

For the transient analysis, the *a posteriori* error variance of the residuals is given by

$$s_0^2 = \frac{S(\mathbf{x})}{M - N} \quad (17)$$

where  $N$  is the number of parameters, and  $S(\mathbf{x})$  is the objective function at its minimum. The variances of the estimated parameters are the diagonal elements of the covariance matrix  $\mathbf{C}_{xx}$ .

$$\mathbf{C}_{xx} = s_0^2 \cdot (\mathbf{J}^T \cdot \mathbf{C}_{zz}^{-1} \cdot \mathbf{J})^{-1} \quad (18)$$

where  $\mathbf{J}$  is the  $M \times N$  Jacobian matrix with the partial derivatives of the residuals at the minimum of Eq. (11) with respect to the unknown parameters  $\mathbf{x}$ , and  $\mathbf{C}_{zz}$  is an  $M \times M$  diagonal matrix with *a priori* error variances  $\sigma_i^2$ . In order to compare the uncertainties among the parameters  $D_{er}$ ,  $t \rightarrow$  and  $\sigma$ , the relative errors  $\sigma_x/x$  are evaluated.

### 3. In-diffusion and out-diffusion experiments without solution sampling

#### 3.1. Material

The experiments were performed on siliceous and diatomaceous mudstones, taken at depths of 618 m and 403 m from the marine Wakkanai and Koetoi formations in the Horonobe research area of Japan, where the Japan Atomic Energy Agency (JAEA) has been operating an Underground Research Laboratory (URL) for research and development related to the geological disposal of high-level radioactive waste (Matsui et al., 2007). Hama et al. (2007) have investigated the *in-situ* chemical conditions and the residence time of groundwater in that area, showing the Na-Cl dominated water chemistry at the depths lower than 250 m. They concluded that the vertical and lateral salinity gradients can be used to test groundwater flow models. Kurikami et al. (2008) investigated the heterogeneity in hydraulic conductivity of both the Wakkanai and Koetoi formations. According to Kurikami et al. (2008), the effective porosity and hydraulic conductivity of the Wakkanai formation range from 0.33 to 0.45 and from  $4 \times 10^{-13}$  to  $3 \times 10^{-11}$  m/s, respectively, and those of the Koetoi formation range from 0.53 to 0.66 and from  $2 \times 10^{-11}$  to  $5 \times 10^{-10}$  m/s, respectively. Given the low conductivity values, diffusion through the matrix is considered the dominant migration process of salinity in both the Wakkanai and Koetoi formations.

Laboratory experiments were performed to estimate NaCl diffusion parameters of the Wakkanai and Koetoi mudstones. While preliminary results of these experiments are presented here, the primary objective of this study is to evaluate the ability of an axisymmetric diffusion experiment to estimate isotropic and anisotropic diffusion parameters with sufficient accuracy. As a secondary objective, these parameter should be estimated using a test that is considerably shorter than a standard through-diffusion experiment.

The drill cores used for laboratory testing showed salt precipitation on their dry surfaces. Dilution experiments were performed to determine the concentrations of  $\text{Na}^+$  and  $\text{Cl}^-$  ions in the cores. The cylindrical samples with a diameter of 50 mm and length of 25 mm were taken from the drill cores using a diamond drill bit and tap water as the drilling fluid, and then immersed in deionized water. The Wakkannai and Koetoi mudstone samples were immersed for 31 and 24 days, respectively. During the first 14 days of the dilution experiments, the dilution waters accommodating the rock samples were vacuumed. The concentrations of  $\text{Na}^+$  and  $\text{Cl}^-$  reached almost constant values within 5 days for both rock samples. The dissolved ions in the diluted water were  $\text{Na}^+$ ,  $\text{Cl}^-$ ,  $\text{F}^-$  and minor quantities of other ions. The porosities of the Wakkannai and Koetoi mudstones were measured by the mercury intrusion method using the remains of drill cores from which the samples were taken, and were estimated to be 0.34 and 0.52, respectively. Using the estimated porosity, equivalent NaCl concentrations of the original porewater were estimated as 0.28 and 0.33 M for the two mudstones. After the dilution experiments, the Wakkannai and Koetoi mudstone samples were immersed for 14 days in one liter of 0.2 and 0.33 M NaCl solution in an incubator held at a constant temperature of 25°C.

### 3.2. Method

Diffusion experiments were performed using the experimental setup shown in Fig. 2, which consists mainly of an acrylic solution reservoir, magnetic stirrer, refractive index sensor and its signal conditioner, an incubator, and personal computer. Eq. (9) indicates that a large solution reservoir results in small changes in tracer concentration during the experiment using a sorptive tracer. To obtain a measureable concentration change in response to the diffusion process, the acrylic solution reservoir was designed to be as small as possible. Salinity was measured using a small fiber optic refractive index sensor (FISO Technologies, Inc.; see Fig. 2(a)). The resolution and the accuracy of the refractive index are 0.00005 and  $\pm 0.0005$  RI, respectively. The acquisition rate was set at 2 Hz. The refractive index was calibrated against NaCl solutions of 0.1 to 0.8 M and showed an almost linear relationship to NaCl concentration over the entire measurement range. The resolution and accuracy of NaCl measurements by the refractive index sensor are 0.005 and 0.05 mol/L. While these values are relatively high, the refractive index sensor was chosen because of the small dimensions of the device, which allowed the solution reservoir to have a small volume for increased concentration changes in response to in- or out-diffusion of

the tracer. The magnetic stirrer is a potential heat source; thus, an incubator with a temperature accuracy of  $\pm 0.2$  °C was used to reduce the temperature variation of the reservoir solution during the experiment.

The in-diffusion experiment was performed on the Wakkanai mudstone, whereas the out-diffusion experiment was performed on the Koetoi mudstone. In the in-diffusion experiment, after assembling the solution reservoir shown in Fig. 2 (a), 17.5 mL of 0.4 M NaCl solution was injected into the reservoir. In the out-diffusion experiment, the 0.33 M NaCl solution, in which the rock sample was immersed before the experiment, was diluted with deionized water by 25%, and then 17.5 mL of the diluted solution was injected into the reservoir. In both experiments, the assembled reservoir was placed on the magnetic stirrer in the incubator, in which the temperature was controlled at 25 °C. The varying reservoir NaCl concentrations were monitored. The experiments were terminated after the changes of the reservoir tracer concentrations approached the level of measurement noise.

### 3.3. Results

Fig. 3 shows the measured NaCl concentrations in each experiment. The changes in concentrations were significantly higher than the measurement resolution, capturing the transient behavior at the beginning of the experiments. These data were interpreted by the steady-state and transient analyses using Eqs. (10) and (11), respectively. The transient analysis using Eq. (11) was performed in two steps. The radial diffusion coefficient,  $D_{er}$ , and capacity factor,  $\tau$ , were first determined assuming isotropic diffusion, i.e.,  $\tau = 1$ , and then all the parameters were determined by the anisotropic diffusion model, using the results of the first analysis as the initial estimates. In the transient analyses, the concentration measurement accuracy of 0.05 mol/L was used as the standard deviation  $\sigma_c$  in Eq. (11). The uncertainties of each parameter were estimated for the steady-state and transient analyses using Eqs. (16) and (18), respectively. The estimated error variances were calculated by Eq. (17).

The fitted curves derived from the transient analyses agree well with the measured tracer concentrations, as shown in Fig. 3. In each experiment, the anisotropic diffusion model slightly reduced the values of the objective function defined by Eq. (11) with  $D_{er}$  and  $\tau$  values different from those obtained from the isotropic diffusion model. However, the curves calculated from the anisotropic diffusion model were almost identical to those from

the isotropic diffusion model (not shown in figures).

Table 1 summarizes the conditions and results of the parameter estimations for each experiment. The capacity factors determined from the transient analysis for the Wakkanai mudstone are consistent with those estimated by the steady-state analysis. Moreover, they are also close to the porosity measured by the mercury intrusion method. This implies that the amount of tracer sorbed onto the pore surface is relatively small compared to that in the porewater. This is expected, since the experiments were performed with high background concentrations  $C_{in}$ . However, for the Koetoi mudstone, the transient analysis yielded capacity factors that were about 20% larger than those estimated from the steady-state analysis and the porosity measured by the mercury intrusion method. This may be explained by the nonlinear release rate of NaCl from the rock sample due to the large reduction in ionic strength in the reservoir solution at the beginning of experiment, as reported for  $Cs^+$  in granite by Samper et al. (2010). In contrast, a constant release rate is assumed in the model, which may lead to a bias in the capacity factor estimated from the transient analysis using the anisotropic model.

For the Wakkanai mudstone, the uncertainties of the capacity factor estimated from the transient analysis are relatively small compared to those for the Koetoi mudstone, which can be compared by the relative error  $\frac{\sigma}{\mu}$  in Table 1. However, the uncertainties of diffusion parameters,  $D_{er}$  and  $\lambda$ , are both very large, though they are relatively small compared to those for the Koetoi mudstone, which can be compared by their relative errors  $\frac{\sigma_{D_{er}}}{D_{er}}$  and  $\frac{\sigma_{\lambda}}{\lambda}$  in Table 1. This indicates that the uncertainties in the estimated diffusion parameters are increased by the application of an anisotropic model. In addition, the goodness-of-fit criterion shows that the model fit to the data from the Koetoi mudstone was slightly worse than that to the data from the Wakkanai mudstone, which increases the estimation uncertainty proportionally.

The values of  $\lambda$  indicate that the Wakkanai mudstone may be almost isotropic, and the Koetoi mudstone is anisotropic; however, the uncertainties of  $\lambda$  are too large to substantiate such a conclusion. Therefore, the diffusion anisotropy of these materials should be further investigated using different experimental configurations, such as the interpretation of concentration profiles in the rock sample. Assuming the isotropic diffusion model, the effective diffusion coefficients of NaCl for the Wakkanai and Koetoi mudstones is  $1.69 \times 10^{-10}$  and  $1.81 \times 10^{-10}$ .

## 4. In-diffusion experiment with solution sampling

### 4.1. Material

An in-diffusion experiment with solution sampling was performed using a fine-grained sandstone, taken at Shirahama, Wakayama prefecture in Japan. The Shirahama sandstone has been used as representative sandstone in Japan for rock mechanical and permeability experiments, in the context of geological storage of CO<sub>2</sub> and radioactive waste (e.g., Zhang et al., 2000; Xue et al., 2005). According to Zhang et al. (2002), the effective porosity of the Shirahama sandstone is about 0.13, and the hydraulic conductivity ranges from 10<sup>-9</sup> to 10<sup>-8</sup> m/s. The mineralogical composition of the Shirahama sandstone is 30.8% quartz, 24.6% illite, 18.4% plagioclase, 8.6% opal, 4.6% lithic materials and other minerals (Kodama et al., 2005). There are a few studies on the diffusion parameters of this material. Sato (2003) investigated the effects of ionic strength and tracer concentration on diffusion of Cs<sup>+</sup> in the Shirahama sandstone, and determined the diffusion and sorption parameters by 1D diffusion experiments. He also measured the cation exchange capacity of the Shirahama sandstone to be 5.84×10<sup>-5</sup> mol/g. Nakashima et al. (2008) estimated the diffusion anisotropy ratio of the Shirahama sandstone to be 0.6, from the X-ray computed tomography-based random walk simulation assuming conservative species.

The main objective of the current study is to test the analytical model against the axisymmetric diffusion experiment with solution replacement, and to examine the applicability of the anisotropic model as well as the isotropic model. We use KBr as the tracer solution, and focus on the diffusion of Br<sup>-</sup> into the rock sample, because Br<sup>-</sup> is usually considered a conservative tracer with a zero sorption coefficient or one that is significantly lower than that of K<sup>+</sup> (Levy and Chambers, 1987).

### 4.2. Method

A cylindrical sample (diameter 50 mm, length 25 mm) was cored from a rock block as described in Section 3.1, with the sample axis perpendicular to the bedding plane. The rock sample was first immersed in deionized water and vacuumed to remove the air in the porespace. The hydration water was used as the reservoir solution in the subsequent diffusion experiment. During the saturation process, the rock sample was weighted and vacuumed until the weight stabilized. From the initial and final weights in the eight-day



saturation process, the effective porosity was estimated as 0.12.

As discussed above, the reservoir volume, the sampling volumes and the number of solution samples taken should be set as small as possible. In this experiment, the volumes of the reservoir and solution replacements were selected to be 20 and 0.1 mL, respectively.

In the diffusion experiment, the rock sample and 20 mL of the hydration water were first put in a PFA bottle. Then, the experiment started by replacing the reservoir solution of 0.2 mL with an equal volume of 0.1 M KBr solution, and the bottle accommodating the rock sample and solution was placed in the incubator. To obtain a uniform distribution of  $\text{Br}^-$  and  $\text{K}^+$  ions in the reservoir during the experiment, the bottle was rotated at 5 rpm using a motor placed outside the incubator, as shown in Fig. 4. At each sampling, 0.1 mL of reservoir solution was taken and replaced with an equal volume of deionized water. The concentrations of  $\text{Br}^-$  and  $\text{K}^+$  of the sample solutions were measured by ion chromatography. For the chemical analyses by ion chromatography, each solution sample was diluted with deionized water to the minimum volume of 0.4 mL needed for analysis. Concentrations of 0.05 mM  $\text{Br}^-$  and 0.03 mM  $\text{K}^+$  were measured, with an estimated uncertainty of 0.6 and 11%, respectively.

### 4.3. Results

Fig. 5 shows the tracer concentrations in the reservoir as a function of time. The effect of solution sampling, which results in a stepwise reduction in reservoir concentration at each sampling time, is more pronounced for  $\text{Br}^-$  than for  $\text{K}^+$ , because the value of  $\downarrow_{s,i}$  for the conservative tracer tends to be larger than that for the sorptive tracer  $\text{K}^+$ , and large  $\downarrow_{s,i}$  accentuates the dilution effects as is evident from Eq. (9). The measured tracer concentrations were interpreted by the steady-state and transient analyses using Eqs. (10) and (11), respectively, considering the sampling terms in Eqs. (7) and (10), following the same approach as discussed above. In the transient analyses using both the isotropic and anisotropic models, the standard deviations in Eq. (11) were assumed to be 3% of the measured concentration for each solution sample. The analytical models were also applied without considering the sampling effects implemented in Eqs. (7) and (10) to examine their significance.

In Fig. 5, the fitted curves derived from the transient analyses agree well with the measured tracer concentrations except for the  $\text{Br}^-$  curve fitted by Eq. (7) without the sampling terms.

Similar to the previous results, the curves calculated from the anisotropic diffusion model were almost identical to those from the isotropic diffusion model, with a slightly smaller value of the final objective function.

Table 2 summarizes the conditions and results of the parameter estimation. The capacity factors determined from the transient analysis are consistent with those estimated by the steady-state analysis. The capacity factor estimated for  $\text{Br}^-$  is slightly lower than the effective porosity reported by Zhang et al. (2007), implying that anion exclusion might reduce the effective porosity. Applying the anisotropic model, the uncertainties of capacity factor and diffusion parameters for both  $\text{Br}^-$  and  $\text{K}^+$  tend to be larger than those estimated by the isotropic model as a result of the estimation of an additional parameter,  $\ell$ . Particularly, the estimation uncertainties of  $D_{\text{er}}$  and  $\ell$  of the anisotropic model are large, even though the fitted curves are almost the same as those obtained with the isotropic model, indicating the strong correlation between these two parameters. The diffusion anisotropy ratio  $\ell$  determined for  $\text{Br}^-$  is smaller than the value of 0.6 obtained by Nakashima et al. (2008). The differences may be in part due to the fact that different rock samples, tracers, and experimental approaches were used for the estimation. However, as will be discussed in Section 5.1., the uniqueness of  $\ell$  in the analysis of the reservoir tracer concentration may depend on the aspect ratio and the degree of the diffusion anisotropy of the rock sample, whose relation is represented as the  $\ell$  value in the anisotropic model.

Table 3 summarizes the results of the parameter estimation ignoring the sampling terms in Eqs. (7) and (10). The parameter uncertainties are increased in the results for  $\text{Br}^-$ . This indicates that the sampling dilution effects need to be accounted for when estimating diffusion parameters of conservative tracers as reported for the in-situ experiments (Naves et al., 2010).

## 5. Discussion

The analytical solutions developed for the analysis of axisymmetric diffusion experiments were tested using measured reservoir concentration data. If the isotropic model is used, the effective diffusion coefficient and the capacity factor are determined straightforwardly with relatively high confidence. On the other hand, if the anisotropic model is applied, the diffusion parameters,  $D_{\text{er}}$  and  $\ell$ , are estimated with unacceptably high uncertainties. These

large uncertainties in the diffusion parameter estimates are a result of the expected high correlation in the anisotropic model due to the relation  $=D_{ez}/D_{er}$ . Changing the experimental design may help reduce this correlation, as will be discussed below. In addition, the correlation between parameters also affects the uniqueness of diffusion parameters.

As discussed above, appropriate selection of the reservoir and solution replacement volumes is essential to reduce dilution effects and to obtain measurable tracer concentration changes in response to in- or out-diffusion of tracer. Moreover, the experimental design is constrained by device limitations and requirements for sample analysis. While the axisymmetric diffusion experiments described above considered some of these criteria, they were not optimized for the determination of asymmetric diffusion coefficients. The question arises whether changes in the experimental layout or sample geometry would allow the identification of asymmetric diffusion behavior with sufficiently low estimation uncertainty. To address this question, we generated synthetic concentration data and performed a detailed analysis of sensitivity, uniqueness, correlation structure, and estimation uncertainty by varying appropriate dimensionless parameters that represent a large variety of experimental conditions and a wide range of potential diffusion properties.

### 5.1. Synthetic analysis of parameter identifiability

The parameters to be identified in the axisymmetric diffusion test are the effective diffusion coefficients and the capacity factor. As demonstrated by the experiments, consistent estimates of the capacity factor are obtained from either the steady-state or the transient analyses using the isotropic and anisotropic diffusion models. In order to see if the radial effective diffusion coefficient,  $D_{er}$ , and the diffusion anisotropy ratio,  $\lambda$ , can be uniquely determined from the transient analysis of reservoir tracer concentrations, the objective function defined by Eq. (11) is evaluated using synthetic data, which were generated assuming that (i) an in-diffusion experiment without solution sampling is performed, (ii) the background tracer concentration is zero, i.e.,  $C_{in}=0$ , and (iii) the capacity factor is known from the steady-state analysis. To make the analysis more general, the objective function is reformulated using dimensionless variables and replacing the standard deviation with the coefficient of variation,  $cv$ :

$$S(\hat{\kappa}, \hat{D}_{er}) = \frac{1}{c\nu^2} \cdot \sum_{i=1}^M \left\{ \frac{c_R^*(\tau_i) - c_R(\tau_i; \hat{\kappa}, \hat{D}_{er})}{c_R^*(\tau_i)} \right\}^2 \quad (19)$$

Here,  $c_R^*$  and  $c_R$  are the synthetic, noise-free measurement data and corresponding calculated values in normalized form, and  $\hat{D}_{er}$  and  $\hat{\kappa}$  are the ratios of  $D_{er}$  and  $\kappa$  over their respective true values. To properly weight the early-time, highly transient data against the late-time, near-steady data, it was assumed that concentrations are continuously monitored, and that 19 discrete values are picked for the analysis at 5% intervals over the entire range of the values measured during the course of the transient experiment.

Fig. 6(a) shows the objective function in the  $\hat{\kappa} - \hat{D}_{er}$  plane for the case of  $\downarrow_R=1$  and  $\ell=0.5$  (e.g.,  $\kappa=1$  and  $L/(2 \cdot r_o)=0.5$ ). The objective function is smooth and has a global minimum at the true parameter set, i.e.,  $(\hat{\kappa}, \hat{D}_{er}) = (1.0, 1.0)$ . However, the objective function is not expected to be concave over the entire admissible parameter space. In fact, a saddle point exists at  $(\hat{\kappa}, \hat{D}_{er}) = (0.35, 1.60)$ , made visible by evaluating the objective function along the base of the narrow valley indicated by the white line in Fig. 6(a). This particular cross section, shown in Fig. 6(b), is created by solving multiple one-dimensional minimization problems along the  $\hat{D}_{er}$  axis for different, fixed values of  $\hat{\kappa}$ . It is obvious that a local minimum exists at or beyond the lower bound of  $\hat{\kappa}$  for this specific case. Besides, the objective function around the true parameter set  $(\hat{\kappa}, \hat{D}_{er}) = (1.0, 1.0)$  is elongated, which indicates that the estimation uncertainties for  $\kappa$  and also for  $D_{er}$  are large as a result of the correlation between  $\kappa$  and  $D_{er}$ .

The same analysis is performed for different values of  $\ell$ , ranging from 0.32 to 6.4 with  $\downarrow_R=1$ . Fig. 7(a) shows the lines of minima along the bottom of the valley of the objective function. The objective function values along these lines are shown in Fig. 7(b), with the locations of the local minima indicated by black dots in both figures. It demonstrates that the inverse problem has a unique solution if  $\ell < 0.5$  or  $\ell > 2.0$ . However, in the range  $0.5 \leq \ell \leq 2.0$ , a local minimum exists on either side of the true parameter values. These indicate that the identifiabilities of  $D_{er}$  and  $\kappa$  are dependent of the aspect ratio, along with the diffusion anisotropy ratio, of the rock sample. In other words, the parameter identifiability may be improved to some degree by the selection of the sample aspect ratio, i.e.,  $L/(2 \cdot r_o)$ . Assuming  $0.1 < \kappa < 1$  for a sedimentary rock sample, the  $\ell$  value falls in the range from 2 to 6.4 if the aspect ratio  $L/(2 \cdot r_o)$  is selected as two. Within this range of  $\ell$ , optimal values for

$D_{er}$  and  $\kappa$  may be obtained from the inverse analysis using Eq. (11) with less influence of possible local minima. Although this particular setting for the sample dimensions was not demonstrated in the performed experiments, it may need to be taken into consideration when designing the axisymmetric diffusion experiments.

For the cases with different values of  $\downarrow_R$ , the locations of the local minima were not significantly different from those shown in Fig. 7. The orientation of the main valley and thus the location of the local minima indicate that, in general, the radial diffusion coefficient,  $D_{er}$ , is relatively well constrained, i.e., the estimate is close to the true value even if the parameter search stops at a local minimum. To obtain the optimal values for  $D_{er}$  and  $\kappa$  from the interpretation of the reservoir tracer concentration, it may be essential to use a global minimization algorithm for parameter estimation.

## 5.2. Synthetic analysis of parameter uncertainty and correlation

The analysis of the actual experiments described in Sections 3 and 4 resulted in very large uncertainties of  $\kappa$  and  $D_{er}$ , caused by the strong correlation between  $\kappa$  and  $D_{er}$  as revealed by the topology of the objective function shown in Figs. 6 and 7. In order to examine if the relative errors in the estimation of  $\kappa$  and  $D_{er}$  are inevitably large if the anisotropic model is used, the covariance matrix defined by Eq. (18) is evaluated. To make the analysis more general, the covariance matrix is normalized with respect to a normal matrix of  $\mathbf{X}$  with diagonal components of  $D_{er}$  and  $\kappa$  and the other components of zero:

$$\tilde{\mathbf{C}}_{xx} = s_0^2 \cdot c\nu^2 \cdot \left( (\mathbf{X} \cdot \mathbf{J}_w^T) \cdot (\mathbf{J}_w \cdot \mathbf{X}) \right)^{-1} \quad (20)$$

where  $\mathbf{J}_w$  is the Jacobian matrix  $\mathbf{J}$  weighted by  $C_R^*$ . The product of  $\mathbf{X}$  and  $\mathbf{J}_w$  can be calculated without assigning specific values for  $D_{er}$  and  $\kappa$  by using Eqs. (12) to (14). The components of the normalized covariance matrix are expressed as

$$\tilde{\mathbf{C}}_{xx} = \begin{bmatrix} \left( \frac{\sigma_{D_{er}}}{D_{er}} \right)^2 & \left( \frac{\sigma_{D_{er}-\kappa}}{\sqrt{\kappa} \cdot \sqrt{D_{er}}} \right)^2 \\ \left( \frac{\sigma_{\kappa-D_{er}}}{\sqrt{\kappa} \cdot \sqrt{D_{er}}} \right)^2 & \left( \frac{\sigma_{\kappa}}{\kappa} \right)^2 \end{bmatrix} \quad (21)$$

The correlation coefficient between  $D_{er}$  and  $\kappa$  is then

$$\rho_{D_{er}-\kappa} = \frac{\sigma_{D_{er}-\kappa}}{\sigma_{D_{er}} \cdot \sigma_{\kappa}} \quad (23)$$

For this analysis, we assume that the measurement errors are on average 1% of the measured concentration value, i.e.,  $cv=0.01$ . For a synthetic analysis, the posterior error variance  $s_0^2$  is equal to one. Fig. 8 shows the relative errors in  $D_{er}$  and  $\kappa$  and their correlation for different values of  $\ell$  in the case of  $\uparrow_R=1$ . Fig. 8(a) shows that the relative error in  $D_{er}$  is lower than that of  $\kappa$  in the admissible ranges of  $\ell$ , as expected from the orientation of the main valley of objective function in Fig. 7(a), consistent with the experimental results summarized in Tables 1 and 2. However, the curves for both  $D_{er}$  and  $\kappa$  show peaks at around  $\ell=0.85$ , where the correlation coefficient between these two parameters takes a value close to -1, as shown in Fig. 8(b). (Note that the relative error is infinite at the point where the correlation coefficient is exactly -1.) As  $\ell$  increases, the relative errors in  $D_{er}$  and  $\kappa$  decrease and increase, respectively, since the increase in the dimensionless aspect ratio of sample  $\ell$  makes the radial diffusion component more prominent compared to the vertical component. In summary, anisotropic diffusion parameters cannot be uniquely identified in the range  $0.5 \leq \ell \leq 2.0$  due to the presence of local minima, as shown in Fig. 7(b). Outside this interval, i.e., for  $0.1 < \ell < 0.5$  and  $2.0 < \ell < 10.0$ , the maximum relative error is three (for  $\lambda=10.0$ ). Specifically, if experiments were performed in the range  $0.1 < \ell < 0.5$ , relative errors are less than 70%, a result that may be considered acceptable or an error that can be further reduced if more accurate concentration data were available. Changing  $\uparrow_R$  does not significantly change the shape of the curves and location of the peaks, but the relative errors decrease slightly as  $\uparrow_R$  decreases for a fixed value of  $\ell$ .

### 5.3. Effects of dilution of reservoir solution

In experiments with solution sampling and replacement, the reservoir solution is diluted by the addition of tracer-free replacement fluid. As a result, the reservoir tracer concentration is sharply reduced after each replacement. The effect of dilution continues even after the experiment would have reached steady state if no samples were taken. This makes it difficult to ascertain steady state, resulting in an unnecessarily long experiment. In the actual experiments with solution sampling (Fig. 5), the reservoir tracer concentration indeed kept decreasing until the end of the experiment. Furthermore, the dilution due to solution replacements may also obscure the reservoir tracer concentration changes caused

by the tracer diffusion between the reservoir and the rock sample. Depending on the replacement and reservoir volumes, the effect of dilution may become significant, leading to erroneous estimates of diffusion parameters.

As an approach to ascertain steady state, the steady-state analysis using Eq. (10) may be helpful. Fig. 9 shows the capacity factor,  $\iota \rightarrow$ , estimated from the steady-state analysis of each data point shown in Fig. 5(a). The capacity factor becomes approximately constant after 12 days, i.e., steady state was reached early during the course of the actual experiment. Fig. 9 also shows the capacity factor determined from the transient analysis of all data taken up to a given time. The capacity factors are consistent after 12 days. By repeatedly performing steady-state and/or transient analyses during the experiment, the point at which the estimated parameters become invariant is sufficient to indicate that steady state is actually reached, even though the data themselves may not be constant due to sampling and dilution effects.

However, the uncertainties of the capacity factor estimated from the steady-state analysis tend to be large as the number of solution replacements. The effects of the sampling and reservoir volumes and the capacity factor on the uncertainties are clearly seen by inspecting the logarithmic sensitivities of Eq. (10) with respect to the measured concentrations. The logarithmic sensitivity is a measure of how the relative error in the measurements propagates to the relative error in the estimated parameter. From Eq. (16), this relation in the steady-state analysis can be expressed as

$$\left(\frac{\sigma_\alpha}{\alpha}\right)^2 = \sum_{i=1}^{M-1} \left\{ \left( \frac{C_R(t_i)}{\alpha} \cdot \frac{\partial \alpha}{\partial C_R(t_i)} \right)^2 \cdot \left( \frac{\sigma_i}{C_R(t_i)} \right)^2 \right\} + \left( \frac{C_R(t_M)}{\alpha} \cdot \frac{\partial \alpha}{\partial C_R(t_M)} \right)^2 \cdot \left( \frac{\sigma_M}{C_R(t_M)} \right)^2 \quad (24)$$

The logarithmic sensitivities can be obtained as

$$\frac{C_R(t_i)}{\alpha} \cdot \frac{\partial \alpha}{\partial C_R(t_i)} = \begin{cases} -\frac{c_R(\tau_i)}{c_R(\tau_M)} \cdot \beta_{s,i} & \text{(in - diffusion experiment)} \\ -\left( \frac{c_R(\tau_i)}{c_R(\tau_M)} - \frac{1}{c_R(\tau_M)} \right) \cdot \beta_{s,i} & \text{(out - diffusion experiment)} \end{cases} \quad (25)$$

$$\frac{C_R(t_M)}{\alpha} \cdot \frac{\partial \alpha}{\partial C_R(t_M)} = \begin{cases} -(\beta_R + 1) & \text{(in -diffusion experiment)} \\ -\left(1 - \frac{1}{c_R(\tau_M)}\right) \cdot (\beta_R + 1) & \text{(out -diffusion experiment)} \end{cases} \quad (26)$$

In Eqs. (25) and (26), the logarithmic sensitivities increase as  $\downarrow_{s,i}$  and  $\downarrow_R$  increase. This means that a large sampling or reservoir volume, and a small capacity factor lead to a larger error in the estimated capacity factor.

The effect of the dilution on reservoir tracer concentrations were examined for the in-diffusion experiment with  $\downarrow_R=10^1$  and  $\ell=10^0$ , using Eq. (7). Fig. 10 shows the transient variations of reservoir tracer concentrations where the reservoir solutions are replaced with tracer-free solutions at volumetric ratios of  $\downarrow_{s,i}/\downarrow_R=0, 0.005, 0.05$  ( $V_{s,i}/V_R=0, 0.5\%, 5\%$ ). Obviously, the effect of dilution becomes large when  $\downarrow_{s,i}/\downarrow_R$  is large. In the case where the reservoir solutions are replaced at the volumetric ratio of  $\downarrow_{s,i}/\downarrow_R=0.05$ , the reduction in the reservoir tracer concentration reflects mostly dilution rather than tracer diffusion. A large  $\downarrow_R$  also increases the effect of dilution as the sorption capacity of the rock sample becomes small compared to the amount of tracer in the solution reservoir as defined by Eq. (6). The use of a conservative tracer is prone to large  $\downarrow_R$  values. If this is the case, the volumes of both the reservoir and replacement solutions should be set small to reduce the dilution effect.

#### 5.4. Limitations and possible applications

This study tested the semi-analytical solution derived from Eq. (1), where the diffusion coefficients in the rock sample are assumed homogeneous and constant, against a series of experiments performed under conditions in which “salt-diffusion” or “counter-diffusion” effects (Shackelford and Daniel, 1991a) may become significant. Under these conditions, individual ions diffuse through porewater by preserving the electro-neutrality with the co-diffusing or counter-diffusing ions. Therefore, their diffusion coefficients depend on the ion concentrations in the porewater, which vary with space and time. Although testing the applicability of Eq. (1) to salt- or counter-diffusion experiments is beyond the scope of this study, it should be acknowledged that Eq. (1) is more suitable to “self-diffusion” and “tracer-diffusion” experiments, where a trace amount of solute diffuses and the electrostatic coupling of ion fluxes can be neglected (Shackelford and Daniel, 1991a).

The use of salt as the tracer can also cause fluid fluxes, induced by chemical osmosis and



density driven flow, and thus affect tracer migration. Neglecting these effects may lead to biased parameter estimates (e.g., Rahman et al., 2005; Kirino et al., 2009). Salt intrusion into the pore space causes chemical disequilibrium between the rock surface and porewater, resulting in the production of co- and counter-diffusing ions, and affecting the sorption properties as well as the diffusion of the primary tracer of interest. Therefore, the parameters determined from the developed analytical solutions represent effective values that include the effects of the other processes. The salinity differences between the reservoir and the porewater can also induce swelling of clayey rocks, leading to pore space deformation and eventually the loss of sample integrity. The above discussion does, however, not apply to the axisymmetric diffusion experiment if using isotopic tracers of the chemical composition of the porewater.

The large external surface area in the axisymmetric diffusion experiment is the main advantage that allows one to obtain tracer concentration changes in shorter experimental time. However, a large surface area increases the risk of probing a large damage surface area, which in turn may affect the diffusion parameter estimates.

Tracer profiling at the end of an axisymmetric diffusion experiment may be an alternative method to obtain the diffusion anisotropy ratio using Eq. (8). However, the concentration profiles near steady state, from which the capacity factor could be estimated independently, are almost uniform. This may lead to difficulty in using such profiles to determine the diffusion anisotropy ratio. Therefore, the transient analysis of the reservoir tracer concentration should be taken into account because it provides the preliminary diffusion and sorption parameters and helps infer the tracer distributions in the rock sample by Eq. (8). This helps determine when the experiments can be terminated to obtain the tracer distribution profiles in the rock sample.

The axisymmetric diffusion test has the advantage of measuring the diffusion and sorption parameters of isotropic rocks using relatively short tests compared to the conventional 1D diffusion experiment. Fig. 11 shows the reservoir tracer concentration changes in the axisymmetric and 1D diffusion experiments calculated by analytical solutions. The concentrations of the 1D diffusion experiment were calculated using the analytical solution of Shackelford and Daniel (1991b). The axisymmetric diffusion experiment reaches steady state much earlier, by about a factor of 5 under the conditions described in Fig. 11, than the 1D diffusion experiment.

In the analytical model, the tracer concentration of replacement solution,  $C_{tr,i}$ , is treated as an arbitrary value, allowing tracer addition during the experiment. This increases the flexibility of the experiment in view of obtaining measured data suitable for the transient analysis using Eq. (11). For example, if the tracer concentration decreased rapidly at the early stage of the experiment (see the  $K^+$  concentration in the experiment shown in Fig. 5 (b)), and insufficient data were collected to capture this transient behavior, the analytical model presented in this study enables repeating the experiment without the need to reset the concentration equilibrium in the reservoir and the porewater. Fig. 12 illustrates hypothetical tracer variations where the same amounts of  $K^+$  ions as the initial tracer addition is added to the reservoir in the experiment shown in Fig. 5 (b). The whole data set can also be interpreted by the transient analysis using Eq. (11).

## 6. Conclusions

We proposed a new axisymmetric diffusion test and associated analysis method for determining the anisotropic diffusion and sorption parameters of sedimentary rocks. In order to examine how reliably the reservoir concentration analysis can estimate anisotropic diffusion and sorption parameters, axisymmetric diffusion tests were performed using three types of sedimentary rocks. The in-diffusion and out-diffusion experiments with and without solution replacements demonstrated the flexibility of the axisymmetric diffusion test. The derived semi-analytical solution agreed well with the measured reservoir tracer concentrations. The capacity factors estimated from the transient and steady-state analyses were consistent for each rock sample. The effective diffusion coefficients were determined straightforwardly by the transient analyses using the isotropic model. However, the diffusion anisotropy ratio is correlated to the radial diffusion coefficient in the anisotropic diffusion model, which leads to large estimation uncertainties of these parameters. A series of numerical analyses suggested that the relative errors in the diffusion anisotropy ratio and the radial diffusion coefficients may be acceptably small if the aspect ratio in dimensionless scale falls in the range  $0.1 < \ell < 0.5$  or  $2.0 < \ell < 10.0$ , and if more accurate tracer concentration data were available.

If the estimation accuracy obtained by the reservoir tracer concentration analysis is insufficient, the results of the analysis can be used to approximate the penetration depth of the diffusion front and to determine the optimal time for tracer profiling. Therefore, the

reservoir tracer concentration analysis is still essential even when tracer profiles are taken. Measuring reservoir concentrations in an axisymmetric diffusion experiment coupled with tracer profiling may be a promising approach to estimate diffusion anisotropy of sedimentary rocks with high confidence. This would overcome the potential problems of conventional diffusion experiments, in which different rock samples have to be used, or in which tracer profiles are taken without the support provided by monitoring the amount of tracer diffusing into or out of the rock sample. Note that the current experimental setup and procedure limit the application of axisymmetric diffusion tests to rigid materials.

The experimental procedure for the axisymmetric diffusion test is simple, and the experiment can reach steady state within a shorter time compared to the conventional 1D in- and out-diffusion experiments. Therefore, the axisymmetric diffusion test is also an effective and efficient approach to determine diffusion and sorption parameters for isotropic rocks.

#### **Acknowledgments**

The authors wish to thank Keisuke Maekawa and JAEA for providing the mudstone samples. The constructive comments by three anonymous reviewers and the associate editor are greatly appreciated. The authors also wish to thank Boris Faybishenko and Ian Charles Bourg (LBNL) for fruitful comments and discussions. The last co-author was supported by the U.S. Dept. of Energy under Contract No. DE-AC02-05CH11231.

#### **References**

- García-Gutiérrez, M., Cormenzana, J.L., Missana, T., Mingarro, M., Martín, P.L., 2006. Large-scale laboratory diffusion experiments in clay rocks. *Physics and Chemistry of the Earth* 31, 523-530.
- García-Gutiérrez, M., Cormenzana, J.L., Missana, T., Mingarro, Alonso, U., Samper, J., Yang, Q., Yi, S., 2008. Diffusion experiments in Callovo-Oxfordian clay from the Meuse/Haute-Marne URL, France. Experimental setup and data analyses. 2008. *Physics and Chemistry of the Earth* 33, S125-S130.
- Hama, K., Kunimaru, T., Metcalfe, R., Martin, A.J., 2007. The hydrogeochemistry of argillaceous rock formations at the Horonobe URL site, Japan, *Physics and*

- Chemistry of the Earth, Volume 32, Issue 1-7, p. 170-180.
- Hollenbeck, K.J., 1998. Invlap.m: A matlab function for numerical inversion of Laplace transforms by the de Hoog algorithm. <http://www.isva.dtu.dk/staff/karl/invlap.htm>.
- Ibaraki, M., 2001. A simplified technique for measuring diffusion coefficients in rock blocks. *Water Resources Research* 37, 1519-1523.
- Kabala, Z.J., 2001. Sensitivity analysis of a pumping test on a well with wellbore storage and skin. *Advances in Water Resources* 24, 483-504.
- Kirino, Y., Yokoyama, T., Hirono, T., Nakajima, T., Nakashima, S., 2009. Effect of density-driven flow on the through-diffusion experiment. *Journal of Contaminant Hydrology* 106, 166-172.
- Kodama, N., Akagawa, S., Fujii, Y., Ishijima, Y., 2005. Deformation behaviour of rocks due to freeze-thaw tests and frost heaving tests. *Proc. JSCE, 35th Rock Mechanics symposium*, 50, 271-276 (in Japanese).
- Kurikami, H., Takeuchi, R., Yabuuchi, S., 2008. Scale effect and heterogeneity of hydraulic conductivity of sedimentary rocks at Horonobe URL site. *Physics and Chemistry of the Earth* 33, S37-S44.
- Levy, B.S., Chambers, R.M., 1987. Bromide as a conservative tracer for soil-water studies. *Hydrological Processes* 1, 385-389.
- Matsui, H., Kurikami, H., Kunimaru, T., Morioka, H., Hatanaka, K., 2007. Horonobe URL project – present status and future plans. In: Eberhardt, E., Stead, D., Morrison, T. (Eds.), *Rock Mechanics: Meeting Society's Challenges and Demands*, Taylor & Francis Group, London, pp. 1193–1201. ISBN: 978-0-415-44401-9.
- Nakashima, Y., Kamiya, S., Nakano, T., 2008. Diffusion ellipsoids of anisotropic porous rocks calculated by X-ray computed tomography-based random walk simulations. *Water Resources Research* 44, doi:10.1029/2008WR006853.
- Naves, A., Dewonck, S., Samper, J., 2010. In situ diffusion experiments: Effect of water sampling on tracer concentrations and parameters. *Physics and Chemistry of the Earth* 35, 242-247.

- Novakowski, K.S., van der Kamp, G., 1996. The radial diffusion method 2. A Semianalytical model for the determination of effective diffusion coefficients, porosity, and adsorption. *Water Resources Research* 32, 1823-1830.
- Press, W.H., Teukolsky, S.A., Vetterling, W.T., Flannery, B.P., 1992. *Numerical recipes*. 2nd ed. Cambridge Univ. Press, New York.
- Rahman, M.M., Chen, Z., Rahman, S.S., 2005. Experimental investigation of shale membrane behavior under tri-axial condition. *Petroleum Science and Technology* 23(9), 1265-1282.
- Samper, J., Yang, C., Naves, A., Yllera, A., Hernandez, A., Molinero, J., Soler, J.M., Hernan, P., Mayor, J.C., Astudillo, J., 2006. A fully 3-D anisotropic numerical model of the DI-B in situ diffusion experiment in the Opalinus clay formation. *Physics and Chemistry of the Earth* 31, 531-540.
- Samper, J., Yang, Q., Yi, S., García-Gutiérrez, M., Missana, T., Mingarro, M., Alonso, U., Cormenzana, J.L., 2008a. Numerical modeling of large-scale solid-source diffusion experiments in Callovo-Oxfordian clay. *Physics and Chemistry of the Earth* 33, S208-S215.
- Samper, J., Dewonck, S., Zheng, L., Yang, Q., Naves, A., 2008b. Normalized sensitivities and parameter identifiability of in situ diffusion experiments on Callovo-Oxfordian clay at Bure site. *Physics and Chemistry of the Earth* 33, 1000-1008.
- Samper, J., Ma, H., Cormenzana, J.L., Lu, C., Montenegro, L., Cunado, M.A., 2010. Testing K-d models of Cs<sup>+</sup> in the near field of a HLW with a reactive transport model. *Physics and Chemistry of the Earth* 35, 278-283.
- Sato, H., 2004. Diffusion and migration of ions in sedimentary rock matrix: effects of ionic strength and tracer concentration on diffusion of Cs<sup>+</sup> ions in sandstone. *Proceedings of the 27th International Symposium on the Scientific Basis for Nuclear Waste Management*, 807, 597-602.
- Shackelford, C.D., Daniel, D.E., 1991a. Diffusion in saturated soil. I: Background. *Journal of Geotechnical Engineering-ASCE* 117(3), 467-484.
- Shackelford, C.D., Daniel, D.E., 1991b. Diffusion in saturated soil. II: Results for

- compacted clay. *Journal of Geotechnical Engineering-ASCE* 117(3), 485-506.
- Skagius, K., Neretnieks, I., 1988. Measurements of Cesium and Strontium Diffusion in Biotite Gneiss. *Water Resources Research* 24(1), 75-84
- Soler, J.M., Samper, J., Yllera, A., Hernández, A., Quejido, A., Fernández, M., Yang, C., Naves, A., Hernánd, P., Wersine, P., 2008. The DI-B in situ diffusion experiment at Mont Terri: Results and modeling. *Physics and Chemistry of the Earth*, 33, S196-S207.
- Van Loon, L.R., Soler, J.M., Muller, W., Bradbury, M.H., 2004a. Anisotropic diffusion in layered argillaceous rocks: A case study with opalinus clay. *Environmental Science & Technology* 38, 5721-5728.
- Van Loon, L.R., Wersin, P., Soler, J.M., Eikenberg, J., Gimmi, T., Hernan, P., Dewonck, S., Savoye, S., 2004b. In-situ diffusion of HTO,  $^{22}\text{Na}^+$ ,  $\text{Cs}^+$  and  $\text{I}^-$  in Opalinus Clay at the Mont Terri underground rock laboratory. *Radiochimica Acta* 92, 757-763.
- Wenk, H.R., Voltolini, M., Mazurek, M., Van Loon, L.R., Vinsot, A., 2008. Preferred orientations and anisotropy in shales: Callovo-Oxfordian shale (France) and opalinus clay (Switzerland). *Clays and clay minerals* 56(3), 285-306.
- Xue, Z.Q., Ohsumi, T., Koide, H., 2005. An experimental study on seismic monitoring of a CO<sub>2</sub> flooding in two sandstones, *Energy* 30, 2352-2359.
- Wersin, P., Van Loon, L.R., Soler, J.M., Yllera, A., Eikenberg, J., Gimmi, T., Hernan, P., Boisson, J.Y., 2004. Long-term diffusion experiment at Mont Terri: first results from field and laboratory data. *Applied Clay Science* 26, 123-135.
- Yllera, A., Hernandez, A., Mingarro, M., Quejido, A., Sedano, L.A., Soler, J.M., Samper, J., Molinero, J., Barcala, J.M., Martin, P.L., Fernandez, M., Wersin, P., Rivas, P., Hernan, P., 2004. DI-B experiment: planning, design and performance of an in situ diffusion experiment in the Opalinus Clay formation. *Applied Clay Science* 26, 181-196.
- Zhang, M., Takahashi, M., Morin, R.H., Esaki, T., 2000. Evaluation and application of the transient-pulse technique for determining the hydraulic properties of low-permeability rocks - Part 2: Experimental application, *Geotechnical Testing*

Journal 23(1), 91-99.

Zhang, M., Takahashi, M., Morin, R.H., Endo, H., Esaki, T., 2002. Determining the hydraulic properties of saturated, low-permeability geological materials in the laboratory: Advances in theory and practice, in: Sara, M.N., Everett, L.G. (Eds.), Evaluation and Remediation of Low Permeability and Dual Porosity Environments, ASTM STP 1415. ASTM International, West Conshohocken, pp. 83-98.

## **Tables**

Table 1 Summary of interpretation of axisymmetric diffusion experiments performed on the samples of Wakkanai and Koetoi mudstones.

Table 2 Summary of interpretation of axisymmetric diffusion experiment performed on the sample of Shirahama sandstone.

Table 3 Summary of interpretation of axisymmetric diffusion experiments performed on the sample of Shirahama sandstone ignoring sampling terms in Eq. (7).

## **Figure Captions**

Fig. 1 Schematic of experimental configurations for the axisymmetric diffusion test.

Fig. 2 Schematic of experimental setup for the in- and out-diffusion experiments without solution replacement performed with Wakkanai and Koetoi mudstones.

Fig. 3 Schematic of experimental setup for the in-diffusion experiment with solution replacement performed with Shirahama sandstone.

Fig. 4 Measured and fitted reservoir tracer concentrations for (a) Wakkanai and (b) Koetoi mudstones.

Fig. 5 Measured and fitted reservoir concentrations of (a)  $\text{Br}^-$  and (b)  $\text{K}^+$  in the in-diffusion experiment with solution sampling performed on core of Shirahama sandstone.

- Fig. 6 (a) Contour plot of the objective function (a) in the  $\hat{\kappa} - \hat{D}_{er}$  parameter plane for  $\hat{\downarrow}_R=1$  and  $\ell=0.5$ , and (b) cross section along the valley, showing conditional minima and saddle point.
- Fig. 7 (a) Lines of valley of conditional minima in the  $\hat{\kappa} - \hat{D}_{er}$  parameter plane for  $0.001 < \ell < 0.01$ , and (b) cross section along valley, showing local minima.
- Fig. 8 (a) Relative standard deviations of  $D_{er}$  and  $\hat{\kappa}$  and (b) their correlation coefficient calculated using the synthetic measurement data for  $\hat{\downarrow}_R=10^0$ .
- Fig. 9 Capacity factor,  $\hat{\kappa}$ , estimated from the steady-state analysis of each measured data point shown in Fig. 3 (a), and results of the transient analysis of time-series data up to the measurement time.
- Fig. 10 Sampling and dilution effects on reservoir tracer concentrations in in-diffusion experiment with solution replacement at volumetric rates of  $\hat{\downarrow}_{s,i}/\hat{\downarrow}_R=0, 0.005, \text{ and } 0.05$  with  $\hat{\downarrow}_R=10^1$  and  $\ell=1$ .
- Fig. 11 Evolution of reservoir tracer concentrations for in-diffusion experiments using axisymmetric and 1D test configurations.
- Fig. 12 Reservoir tracer concentration for repeated in-diffusion experiment.



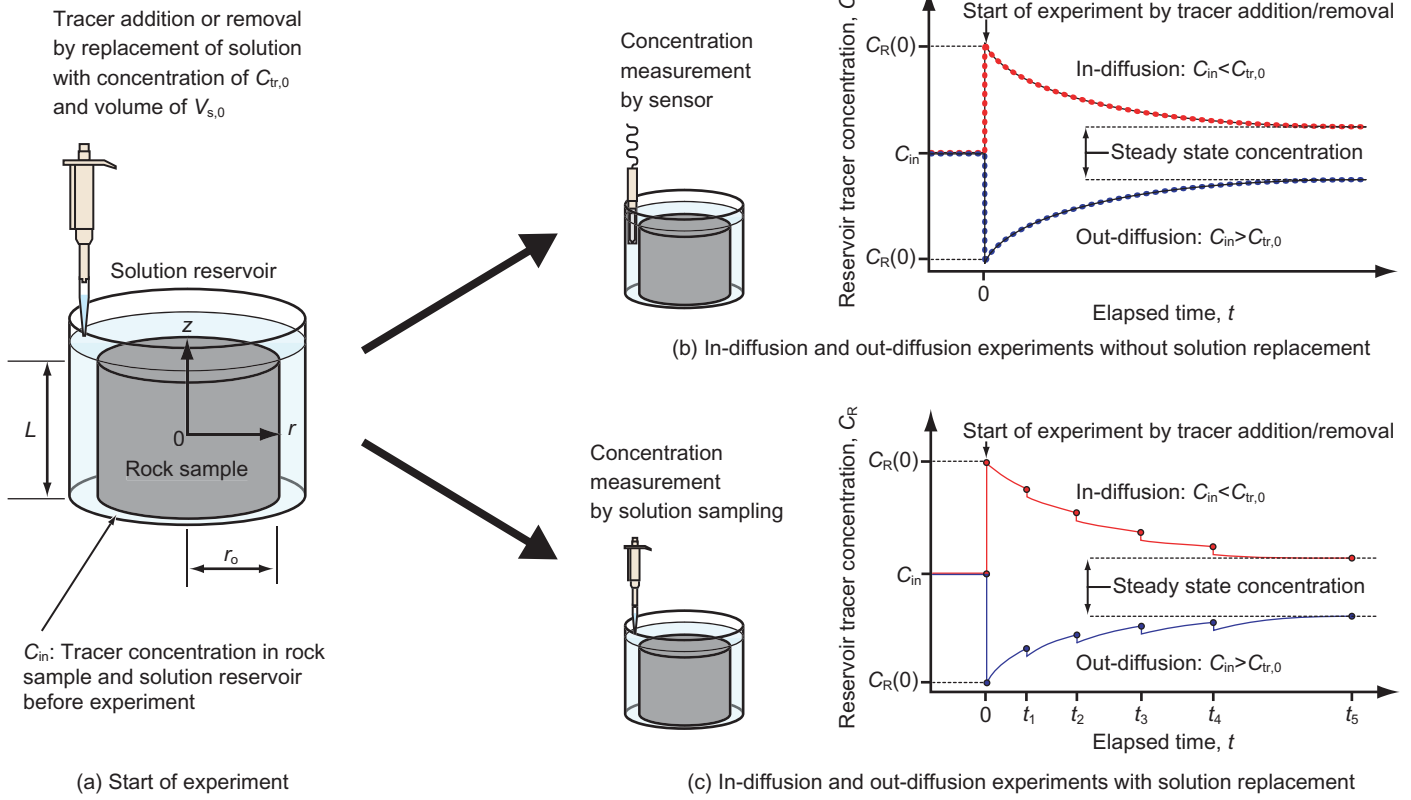
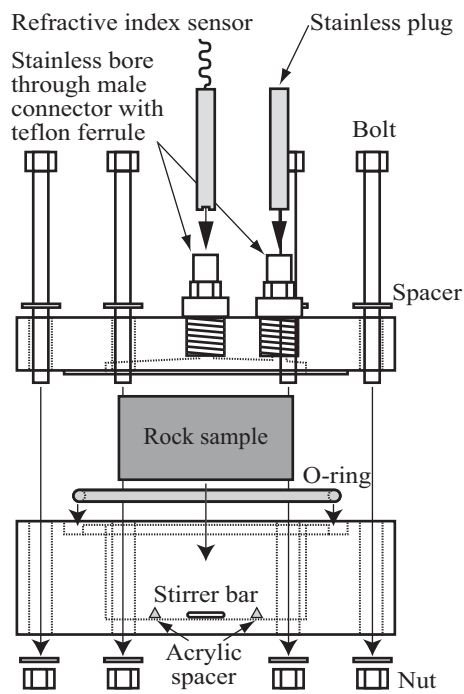
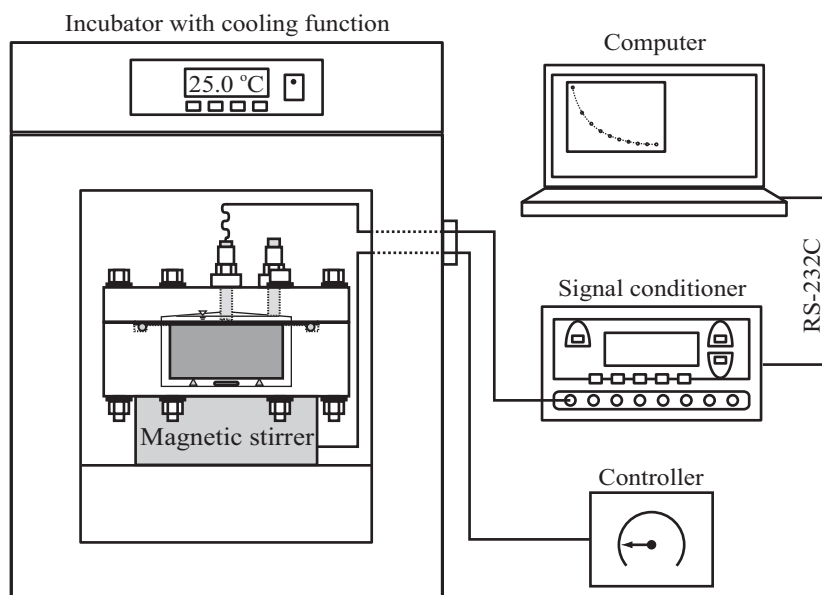


Figure 1



(a) Diffusion cell assembly



(b) Experimental setup for diffusion experiment without solution replacement

Figure 2

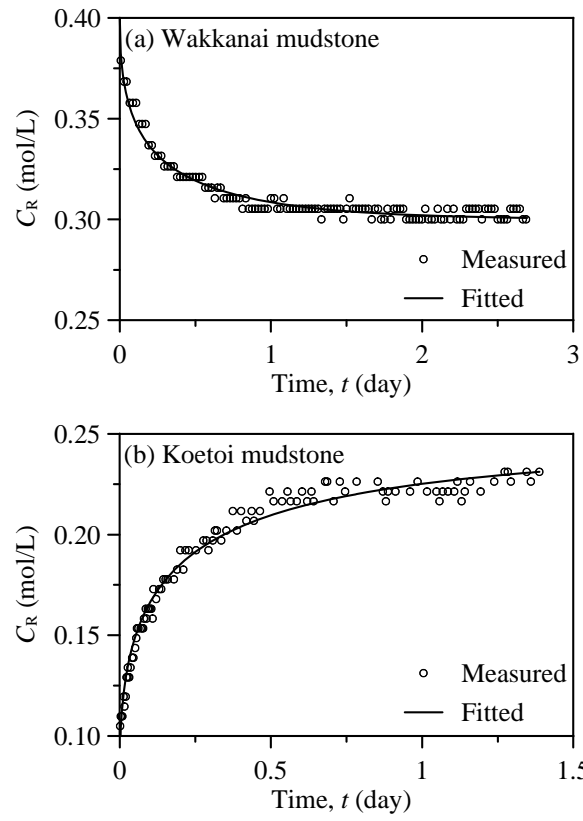


Figure 3

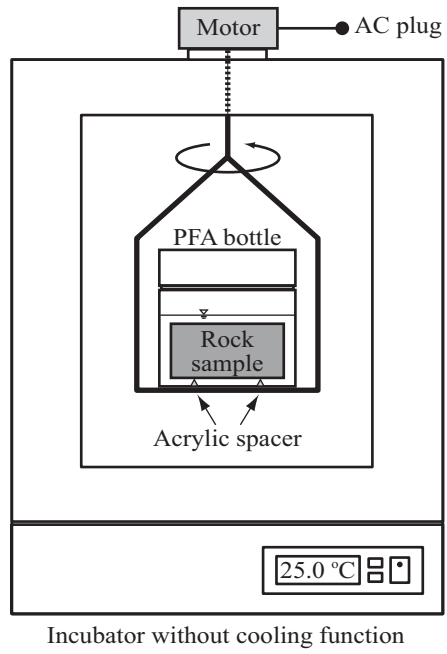


Figure 4

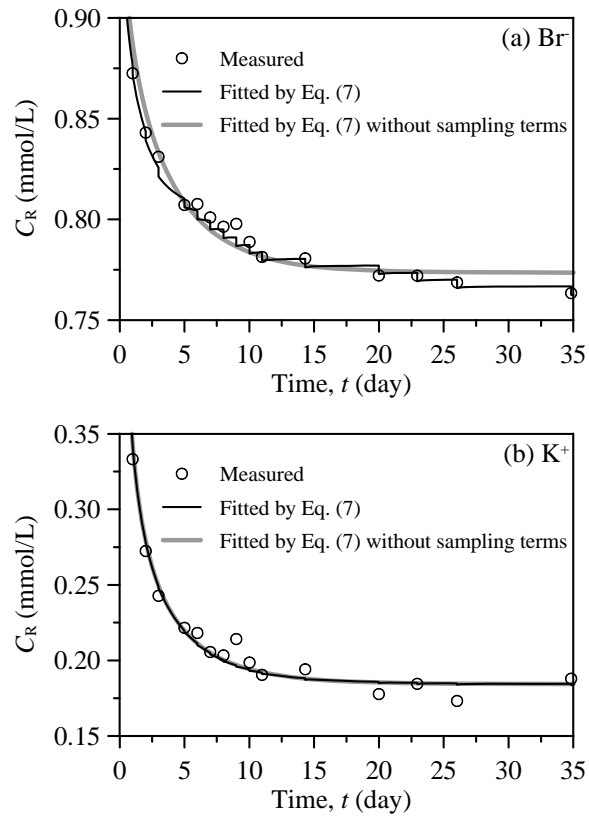


Figure 5

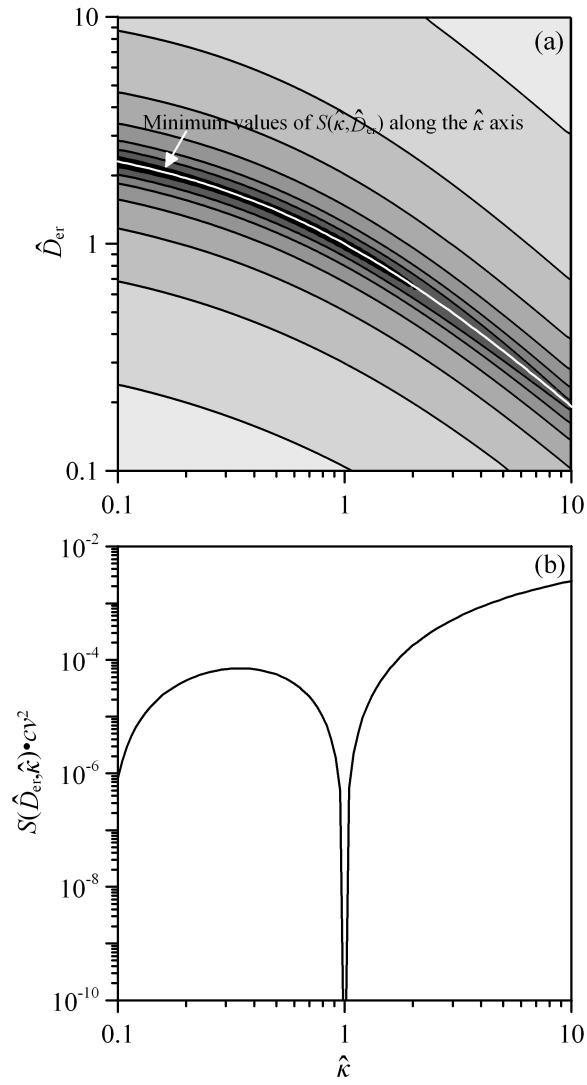


Figure 6

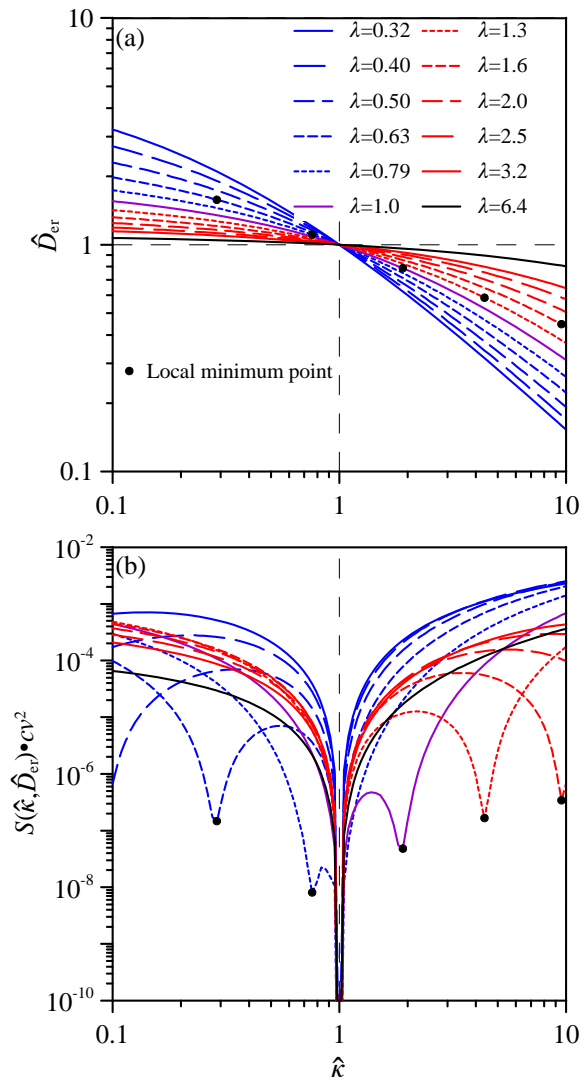


Figure 7

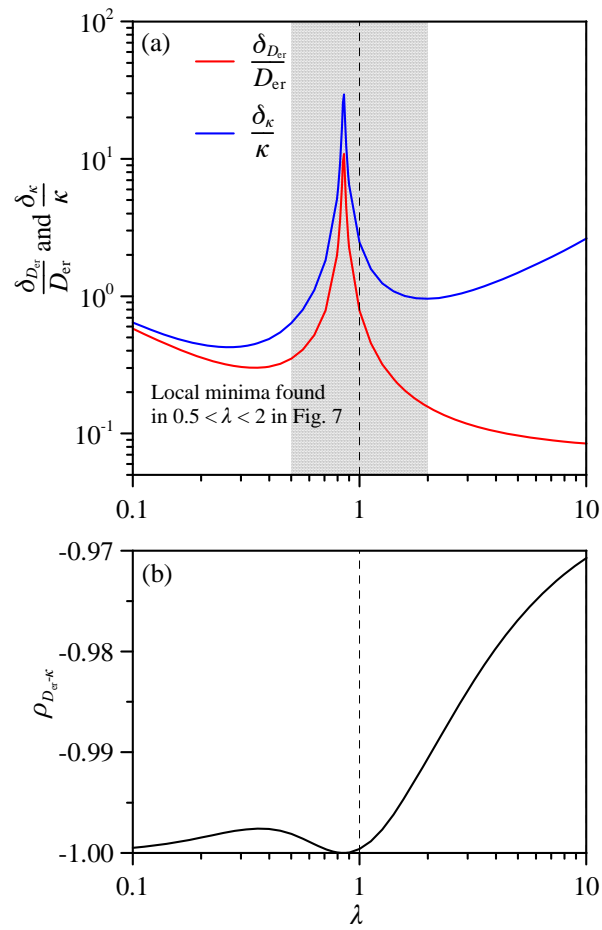


Figure 8



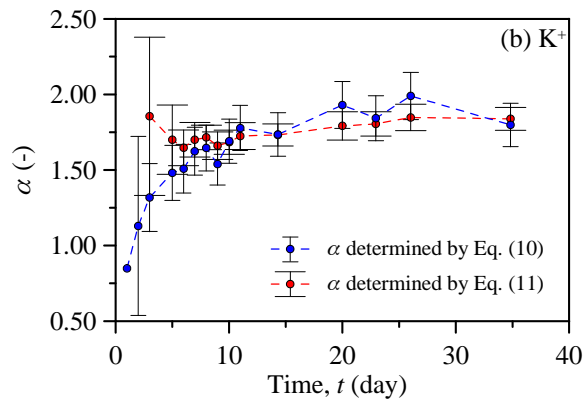
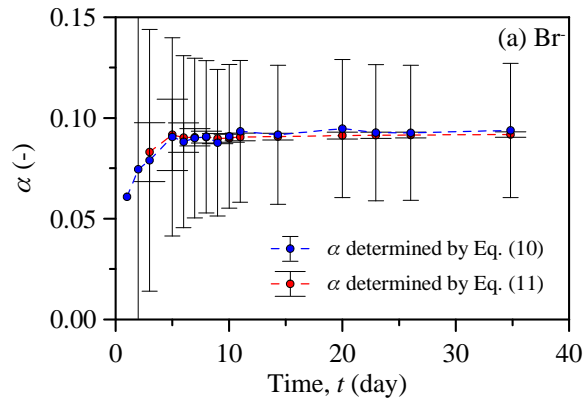


Figure 9

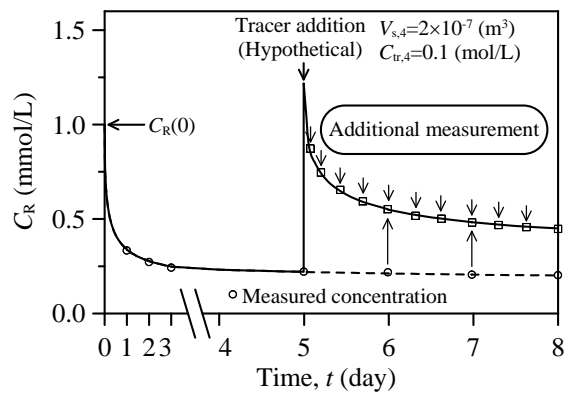


Figure 10

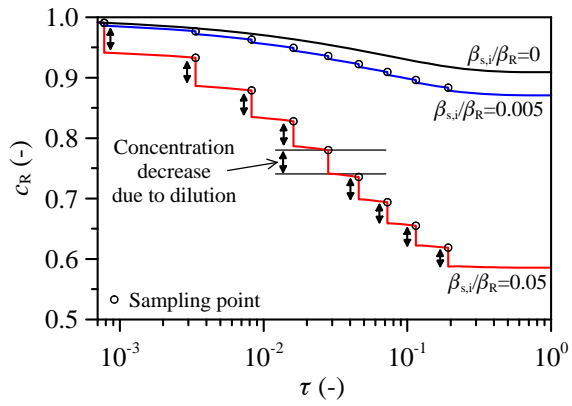


Figure 11

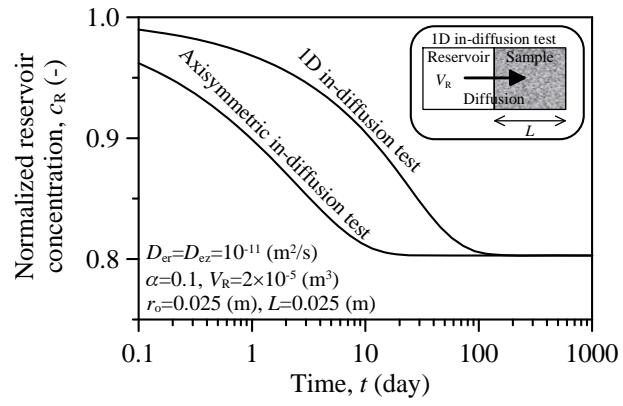


Figure 12

Table 1

Material and method	Rock sample	Wakkanai mudstone			Koetoi mudstone		
	Method	In-diffusion without solution sampling			Out-diffusion without solution sampling		
Tracer	$V_R / V_{s,i}$ (m <sup>3</sup> )	1.75×10 <sup>-5</sup> / -			1.75×10 <sup>-5</sup> / -		
	$C_{in} / C_R(0) / C_{tr,i}$ (mol/L)	0.2 / 0.4 / -			0.33 / 0.08 / -		
Interpretation method	Analysis state	Transient		Steady	Transient		Steady
	Diffusion anisotropy	Isotropic	Anisotropic	n.a.	Isotropic	Anisotropic	n.a.
Estimated parameters	$\sigma_i^*$	0.05 (mol/L)		n.a.	0.05 (mol/L)		n.a.
	$D_{er} \times 10^{10}$ (m <sup>2</sup> /s)	1.69±0.08 <sup>**</sup>	1.68±0.92	-	1.81±0.21	2.12±16.8	-
	$\alpha$ (-)	0.35±0.01	0.35±0.01	0.35	0.64±0.04	0.65±0.72	0.53
	$\kappa$ (-)	1 <sup>***</sup>	1.01±1.00	-	1 <sup>***</sup>	0.78±14.6	-
Goodness of fit	$s_0^2$ (-)	4.06×10 <sup>-3</sup>	4.07×10 <sup>-3</sup>	-	9.77×10 <sup>-3</sup>	9.82×10 <sup>-3</sup>	-
	$\beta_R$ (-)	1.00	1.00	1.00	0.54	0.53	0.65
Dimensionless quantity	$\beta_{s,i} / \beta_R$ (-)	-	-	-	-	-	-
	$\lambda$ (-)	0.50	0.50	-	0.50	0.57	-
	$\sigma_{Der} / D_{er}$ (-)	0.02	0.28	-	0.06	4.01	-
	$\sigma_{\alpha} / \alpha$ (-)	0.01	0.01	-	0.04	0.56	-
	$\sigma_{\kappa} / \kappa$ (-)	-	0.50	-	-	9.54	-

\* $\sigma_i$  was assigned as the accuracy of the concentration measurement by the refractive index sensor

\*\*95% confidence interval

\*\*\* $\kappa$  is treated as 1.0 in the transient analyses using the isotropic diffusion model

Table 2

Material and method	Rock sample	Shirahama sandstone					
	Method	In-diffusion with solution sampling					
	$V_R / V_{s,i} \text{ (m}^3\text{)}$	$2.0 \times 10^{-5} / 1.0 \times 10^{-7}$					
	$C_{in} / C_R(0) / C_{tr,i} \text{ (mol/L)}$	$2.0 \times 10^{-5} / 1.0 \times 10^{-7} / 0.0$					
	Tracer	Br-			K+		
Interpretation method	Analysis state	Transient		Steady	Transient		Steady
	Diffusion anisotropy	Isotropic	Anisotropic	n.a.	Isotropic	Anisotropic	n.a.
	$\sigma_i^*$	$0.03 \times C_R(t_i) \text{ (mol/L)}$		n.a.	$0.03 \times C_R(t_i) \text{ (mol/L)}$		n.a.
Estimated parameters	$D_{er} \times 10^{11} \text{ (m}^2\text{/s)}$	$2.12 \pm 0.28^{**}$	$3.26 \pm 7.64$	-	$11.6 \pm 2.0$	$19.4 \pm 145$	-
	$\alpha \text{ (-)}$	$0.092 \pm 0.001$	$0.092 \pm 0.003$	$0.094 \pm 0.03$	$1.84 \pm 0.08$	$1.85 \pm 0.11$	$1.80 \pm 0.14$
	$\kappa \text{ (-)}$	$1^{***}$	$0.42 \pm 2.45$	-	$1^{***}$	$0.33 \pm 6.78$	-
Goodness of fit	$s_0^2 \text{ (-)}$	$1.83 \times 10^{-2}$	$1.86 \times 10^{-2}$	-	1.57	1.47	-
	$\beta_R \text{ (-)}$	4.62	4.62	4.52	0.23	0.23	0.24
Dimensionless quantity	$\beta_{s,i} / \beta_R \text{ (-)}$	0.005	0.005	-	0.005	0.005	-
	$\lambda \text{ (-)}$	0.50	0.77	-	0.50	0.87	-
	$\sigma_{Der} / D_{er} \text{ (-)}$	0.06	1.08	-	0.08	3.44	-
	$\sigma_{\alpha} / \alpha \text{ (-)}$	0.01	0.01	0.17	0.02	0.03	0.04
	$\sigma_{\kappa} / \kappa \text{ (-)}$	-	2.65	-	-	9.48	-

\* $\sigma_i$  was assumed as 3% of the concentration measured by the ion chromatography

\*\*95% confidence interval

\*\*\* $\kappa$  is treated as 1.0 in the transient analyses using the isotropic diffusion model

Table 3

Material and method	Rock sample	Shirahama sandstone					
	Method	In-diffusion with solution sampling					
	$V_R / V_{s,i}$ (m <sup>3</sup> )	$2.0 \times 10^{-5} / 1.0 \times 10^{-7}$					
	$C_{in} / C_R(0) / C_{tr,i}$ (mol/L)	$2.0 \times 10^{-5} / 1.0 \times 10^{-7} / 0.0$					
	Tracer	Br-			K+		
Interpretation method	Analysis state	Transient		Steady	Transient		Steady
	Diffusion anisotropy	Isotropic	Anisotropic	n.a.	Isotropic	Anisotropic	n.a.
	$\sigma_i^*$	$0.03 \times C_R(t_i)$ (mol/L)		n.a.	$0.03 \times C_R(t_i)$ (mol/L)		n.a.
Estimated parameters	$D_{er} \times 10^{11}$ (m <sup>2</sup> /s)	1.12±0.20**	1.59±7.96	-	11.2±1.9	13.5±27.7	-
	$\alpha$ (-)	0.12±0.01	0.12±0.01	0.13±0.04	1.88±0.08	1.88±0.10	1.83±0.15
	$\kappa$ (-)	1***	0.49±5.53	-	1***	0.69±2.83	-
Goodness of fit	$s_0^2$ (-)	$8.34 \times 10^{-2}$	$7.93 \times 10^{-2}$	-	1.54	1.44	-
Dimensionless quantity	$\sigma_{Der}/D_{er}$ (-)	0.18	5.01	-	0.17	2.05	-
	$\sigma_{\alpha}/\alpha$ (-)	0.03	0.04	0.31	0.04	0.05	0.08
	$\sigma_{\kappa}/\kappa$ (-)	-	11.3	-	-	4.10	-

\* $\sigma_i$  was assumed as 3% of the concentration measured by the ion chromatography

\*\*95% confidence interval

\*\*\* $\kappa$  is treated as 1.0 in the transient analyses using the isotropic diffusion model

## DISCLAIMER

This document was prepared as an account of work sponsored by the United States Government. While this document is believed to contain correct information, neither the United States Government nor any agency thereof, nor The Regents of the University of California, nor any of their employees, makes any warranty, express or implied, or assumes any legal responsibility for the accuracy, completeness, or usefulness of any information, apparatus, product, or process disclosed, or represents that its use would not infringe privately owned rights. Reference herein to any specific commercial product, process, or service by its trade name, trademark, manufacturer, or otherwise, does not necessarily constitute or imply its endorsement, recommendation, or favoring by the United States Government or any agency thereof, or The Regents of the University of California. The views and opinions of authors expressed herein do not necessarily state or reflect those of the United States Government or any agency thereof or The Regents of the University of California.

Ernest Orlando Lawrence Berkeley National Laboratory is an equal opportunity employer.